Supplementary material

WRF-Chem simulated surface ozone over South Asia during the pre-monsoon: Effects of emission inventories and chemical mechanisms

Amit Sharma[1, 2, *], Narendra Ojha[2, *], Andrea Pozzer[2], Kathleen A. Mar[3], Gufran Beig[4], Jos Lelieveld[2, 5], and Sachin S. Gunthe[1]

[1]Department of Civil Engineering, Indian Institute of Technology Madras, Chennai, India
[2]Atmospheric Chemistry Department, Max Planck Institute for Chemistry, Mainz, Germany
[3]Institute for Advanced Sustainability Studies, Potsdam, Germany
[4]Indian Institute for Tropical Meteorology, Pune, India
[5]Energy, Environment and Water Research Center, The Cyprus Institute, Nicosia, Cyprus

[*]Correspondence to Amit Sharma (amit.iit87@gmail.com) and Narendra Ojha (narendra.ojha@mpic.de)

Table S1. Diurnal mean biases (model-observations) in ppbv for all runs at different sites

Site	HTAP-RADM2	INTEX-RADM2	S4RS-RADM2	HTAP-MOZ
Mohali	-3.4	-5.5	-9.4	1.0
Nainital	0.6	-2.0	-1.2	8.3
Pantnagar	17.8	15.1	16.1	24.7
Delhi	-6.5	-5.4	-12.3	-16.0
Dibrugarh	21.6	20.6	16.8	39.1
Kanpur	18.2	11.4	10.0	17.8
Mt. Abu	4.7	3.0	2.0	3.9
Udaipur	11.8	10.3	9.7	11.4
Jabalpur	-10.2	-15.1	-12.4	-2.1
Ahmedabad	8.7	8.1	7.8	3.7
Haldia	13.0	10.0	9.9	25.7
Bhubaneshwar	6.4	4.8	4.8	13.1
Joharapur	9.0	5.1	8.0	12.0
Pune	5.1	2.2	4.7	6.9
Anantpur	-5.3	-12.9	-11.2	4.8
Gadanki	7.1	3.2	3.8	11.6
Kannur	15.7	13.4	12.7	13.6
Thumba/Trivendrum	11.7	9.9	6.1	12.0

Table S2. Noontime (1130-1630 IST) average biases in ppbv for all runs at different sites

Site	HTAP-RADM2	INTEX-RADM2	S4RS-RADM2	HTAP-MOZ
Mohali	-17.6	-20.8	-24.8	-13.5
Nainital	8.1	5.8	6.2	17.0
Pantnagar	10.5	7.4	8.5	20.4
Delhi	-12.3	-21.5	-26.0	-11.3
Dibrugarh	28.8	31.5	24.6	40.7
Kanpur	23.5	12.5	15.7	28.7
Mt. Abu	9.7	7.3	6.5	10.6
Udaipur	9.4	7.5	6.8	10.7
Jabalpur	0.9	-8.0	-2.5	8.8
Ahmedabad	10.7	9.4	6.9	10.7
Haldia	19.4	14.8	14.0	29.3
Bhubaneshwar	10.2	12.2	7.3	19.9
Joharapur	16.5	11.1	14.4	23.1
Pune	10.5	4.4	10.5	15.2
Anantpur	0.2	-10.0	-8.7	13.5
Gadanki	14.6	7.9	8.7	25.2
Kannur	22.5	14.9	15.0	27.4
Thumba/Trivendrum	24.0	19.9	11.1	35.8

Table S3. Diurnal mean biases in ppbv over different region in all model runs

Region	HTAP-RADM2	INTEX-RADM2	S4RS-RAMD2	HTAP-MOZ
North	5.4	2.7	0.6	9.4
East	13.7	11.8	10.5	21.4
West	7.9	5.8	6.4	6.4
Central	-10.2	-15.1	-12.4	-2.1
South	7.3	3.4	2.9	10
Overall	7.0	4.2	3.6	10

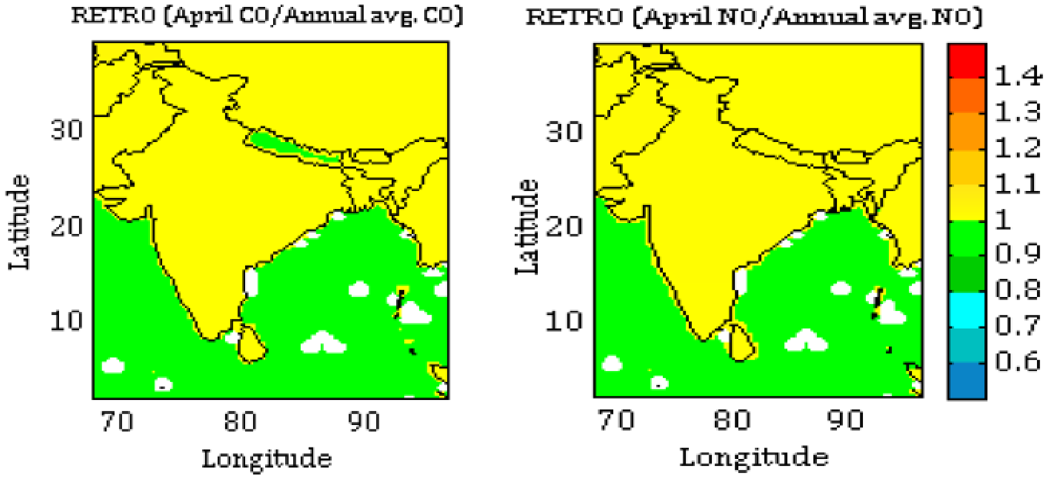

Figure S1. Spatial distribution of ratio of April emissions to annual average emissions for CO (left) and NO (right) derived from the RETRO inventory (http://accent.aero.jussieu.fr/RETRO_metadata.php).

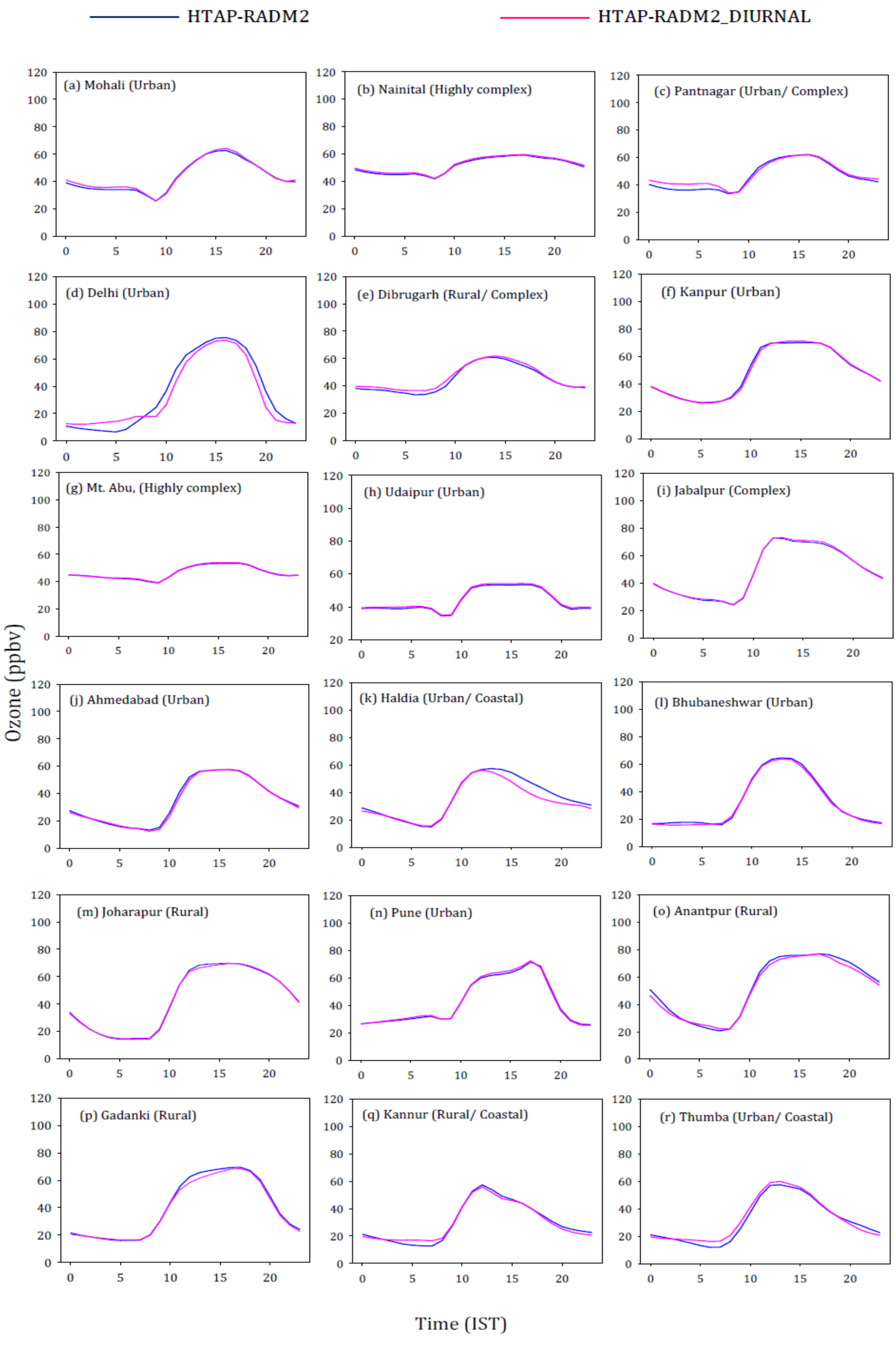

Figure S2. Comparison of 15 day average (01st April, 2013 – 15th April, 2013) diurnal variation of surface ozone simulated for anthropogenic emissions with and without the incorporation of diurnal profile of emissions at various observation sites. Both model simulations are with the HTAP inventory and RADM2 chemistry option.

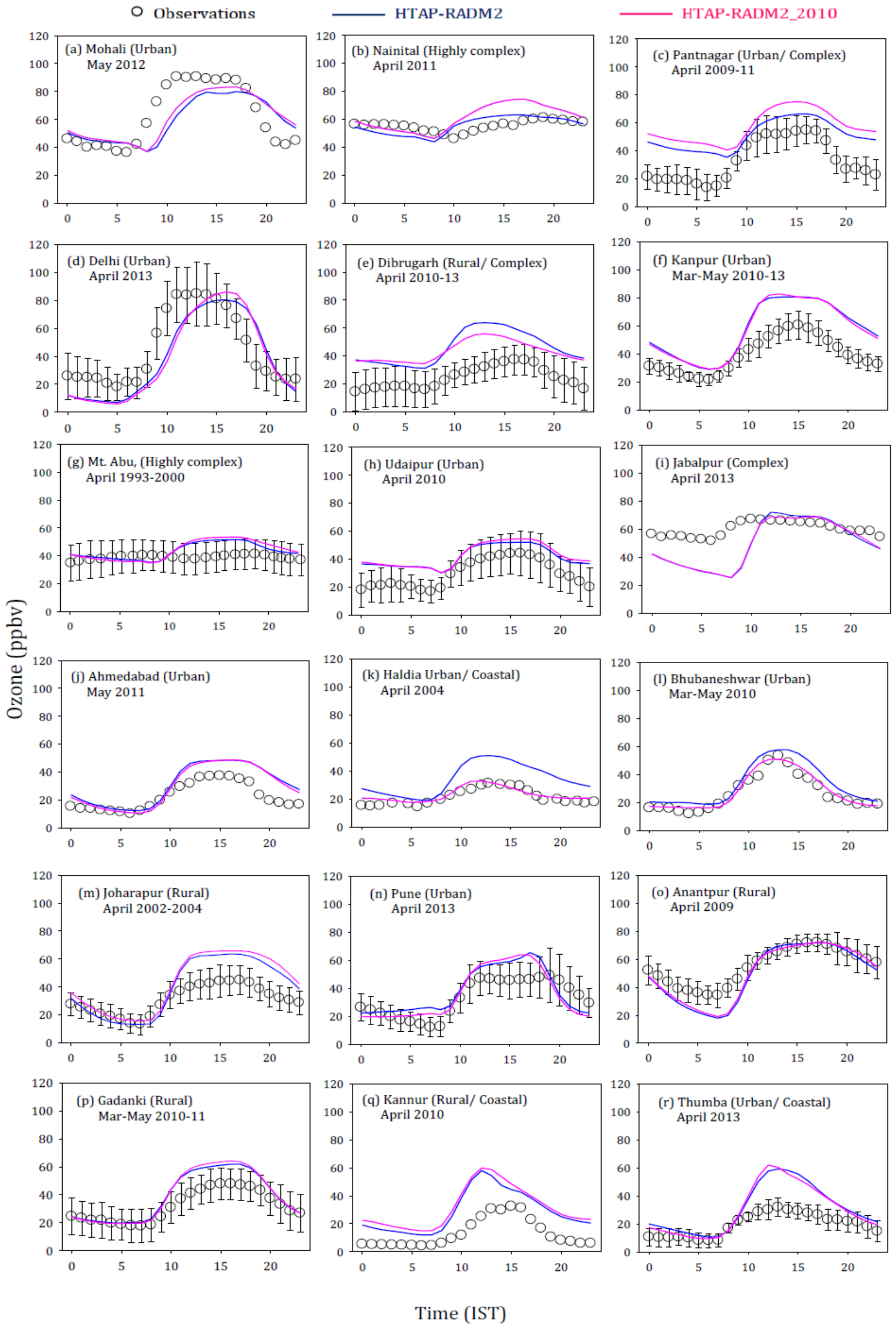

Figure S3. Comparison of monthly average diurnal variation of surface ozone simulated for the years 2010 and 2013 at various observation sites. The observational data is available for the period indicated in the figure. Error bars represent the temporal standard deviation of the monthly averages. All model simulations are with the HTAP inventory and RADM2 chemistry option.

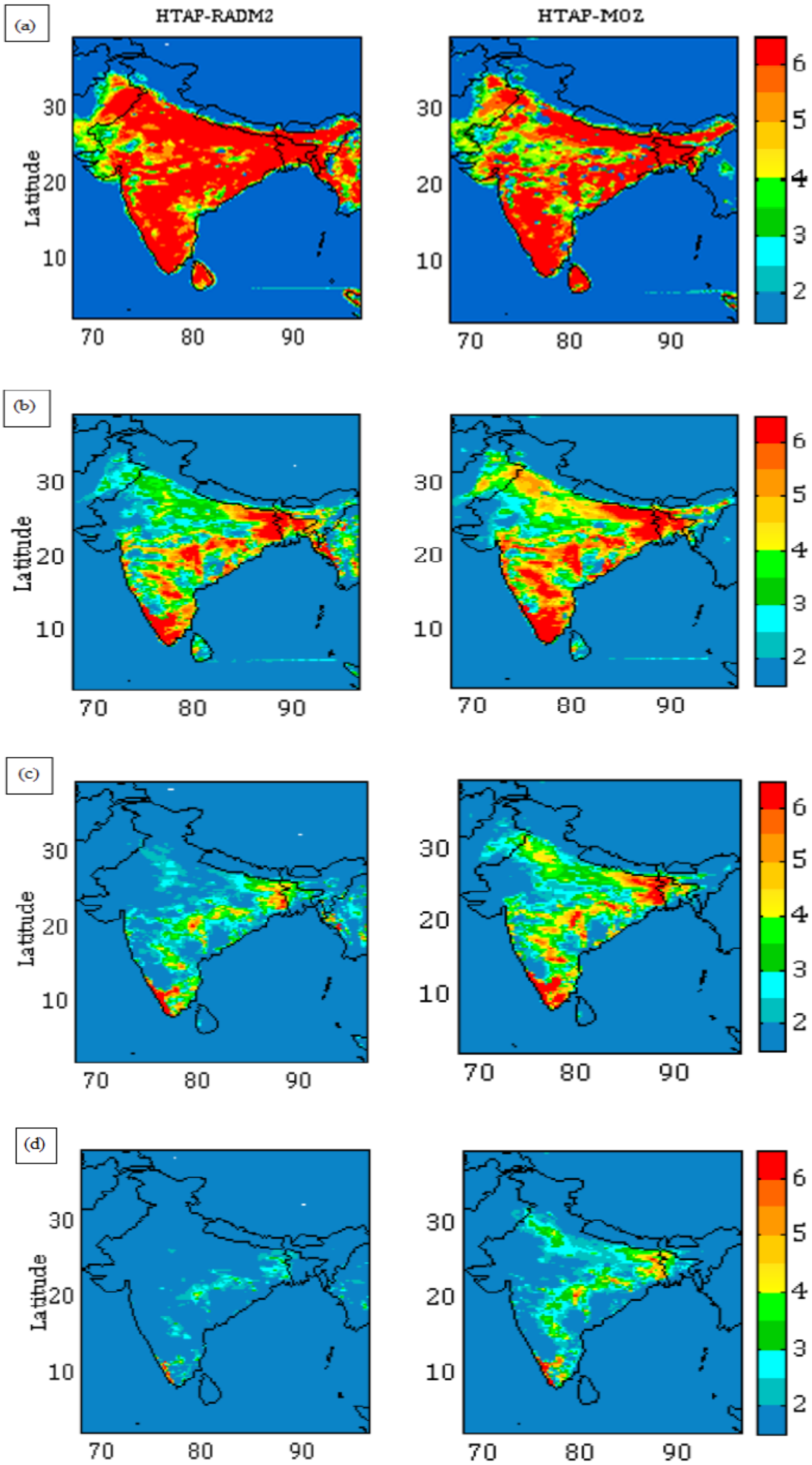

Figure S4. Spatial distribution of net daytime ozone chemical tendency (in ppbv h^{-1}) at model (a)level 1 - surface; (b) level 4; (c) level 5; and (d) level 6 during 0630-1230 IST. The pressure distribution at these model levels is shown in figure S5. Note the colour scale difference with respect to Fig. 9.

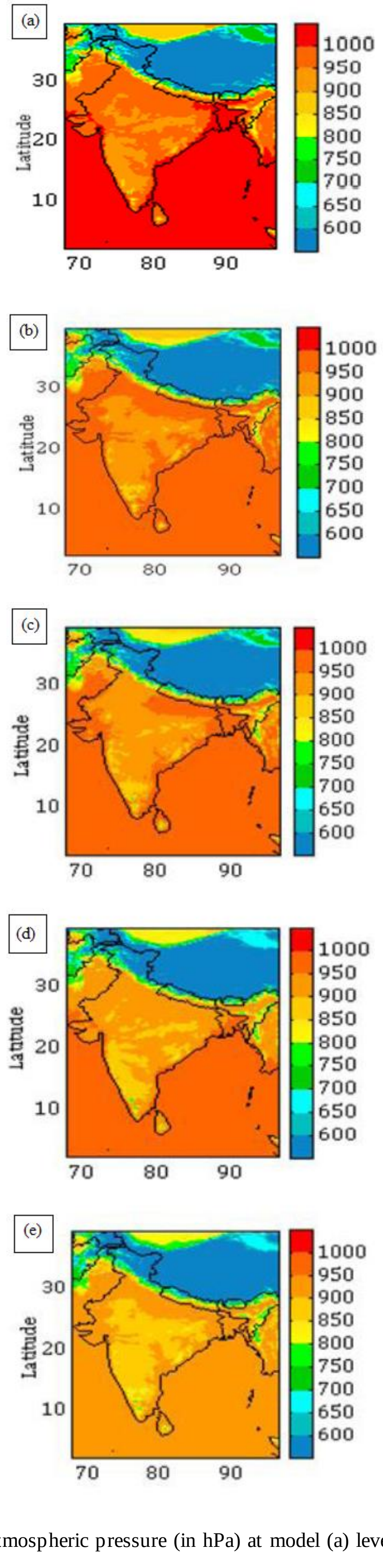

Figure S5. Spatial distribution of atmospheric pressure (in hPa) at model (a) level 1 - surface; (b) level 3; (c) level 4; (d) level 5 and (e) level 6.

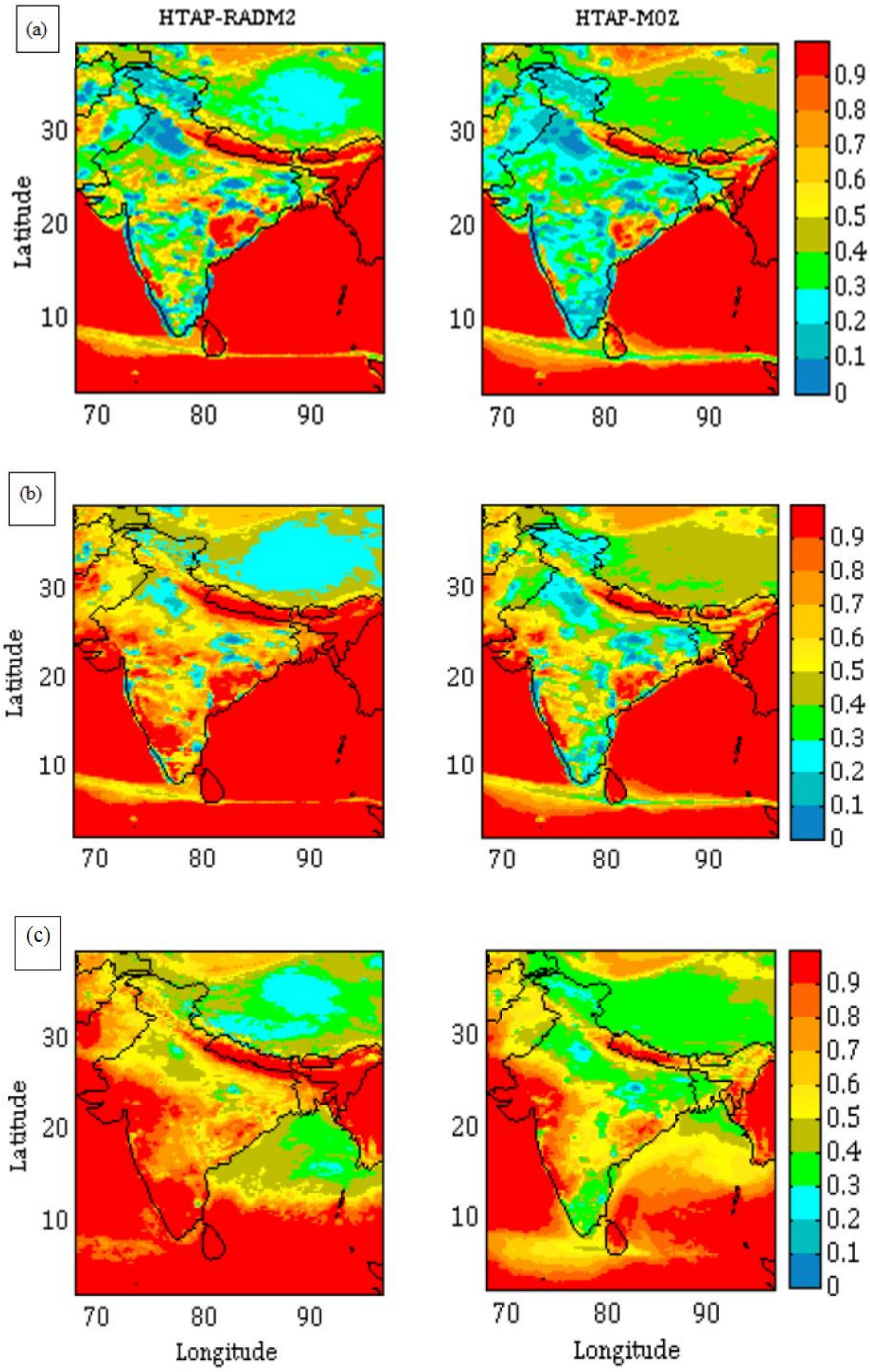

Figure S6. Spatial distribution of daytime (0630-1230 IST) average CH_2O/NO_y ratio comparing simulations with the MOZART and RADM2 chemical mechanisms at model (a) level 1- surface (b) level 3; and (c) level 6 during April. Note the colour scale difference with respect to Fig. 10.